Track Deflection of Intense Tropical Cyclones Past a Mountain Range as Explored by Idealized Simulations

林柏辰、黃清勇

國立中央大學 大氣科學系

2025/09/02

Outline

- Introduction
- Experimental design
- Results
- Conclusions
- Reference

Introduction

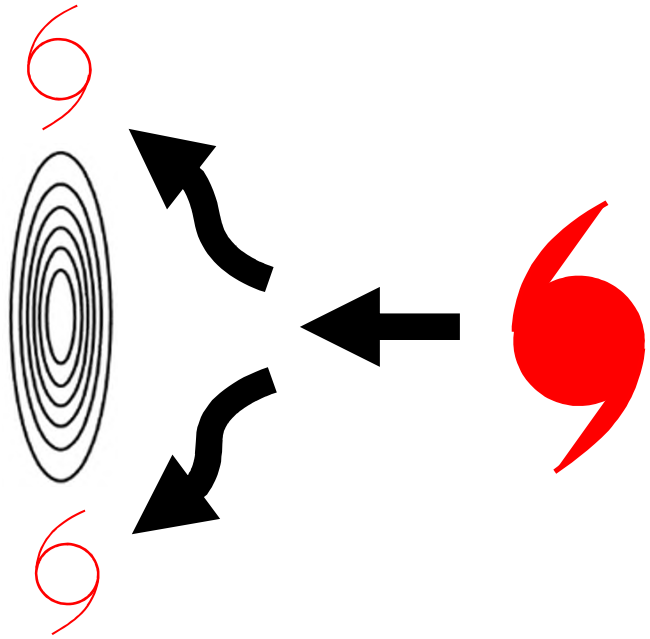

environment

location

intensity

size

steering flow

- When typhoons approach Taiwan, there are significant changes in both the intensity and track of the typhoon, which increase the difficulty of forecasting
- Accurately predicting the intensity and track of typhoons is crucial

Experimental design

WRF Idealize Model : version 3.4.1

Resolution (nested domains)

- D01 (401×401) : 15 km
- D02 (801×801) : 3 km

f-plane : 23.5°

Vertical levels : 41

Model top : 20km

Sea surface temperature : 27°C

Mean flow : 4m/s east wind

Terrain height : 3500m

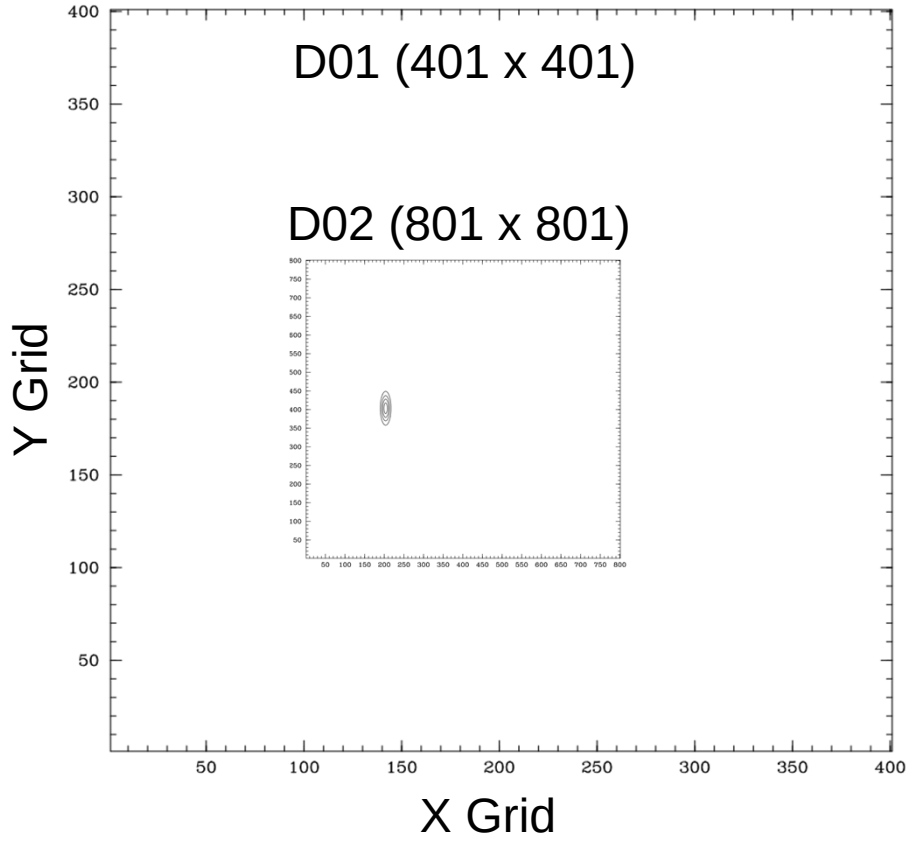

scheme	Idealized
cumulus	Modifed Tiedtke (only for domain1)
microphysics	WSM6-class graupel
planetary boundary layer	YSU
radiation	X

Introduction

The Interaction between Vortex and Terrain

4 terrain angles

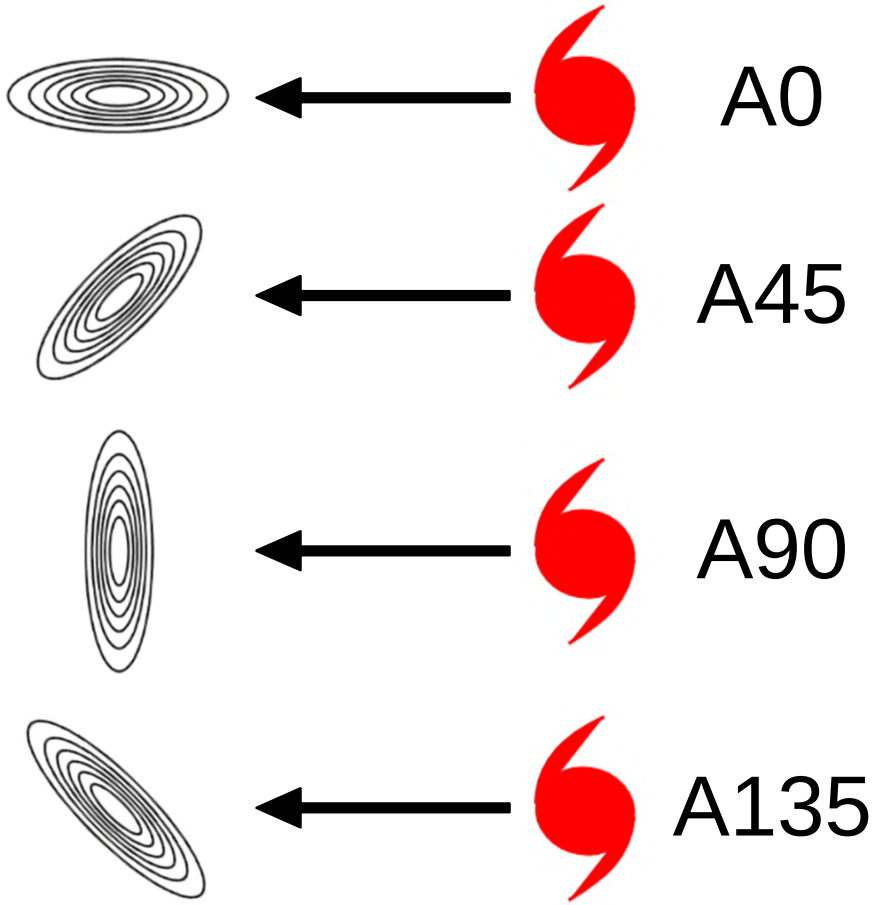

10 departure positions

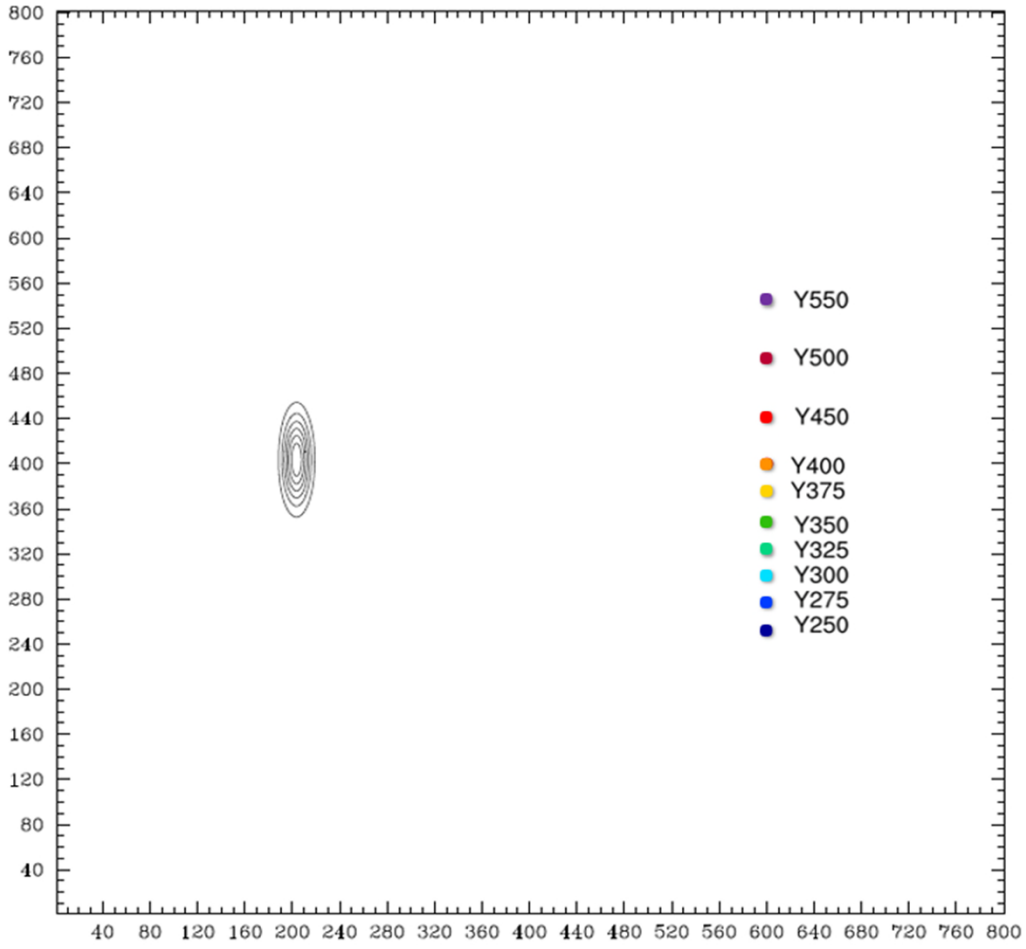

Insert adjusted vortex to pure field

Introduction

Adjusting the initial vortices by incorporating the DVI method

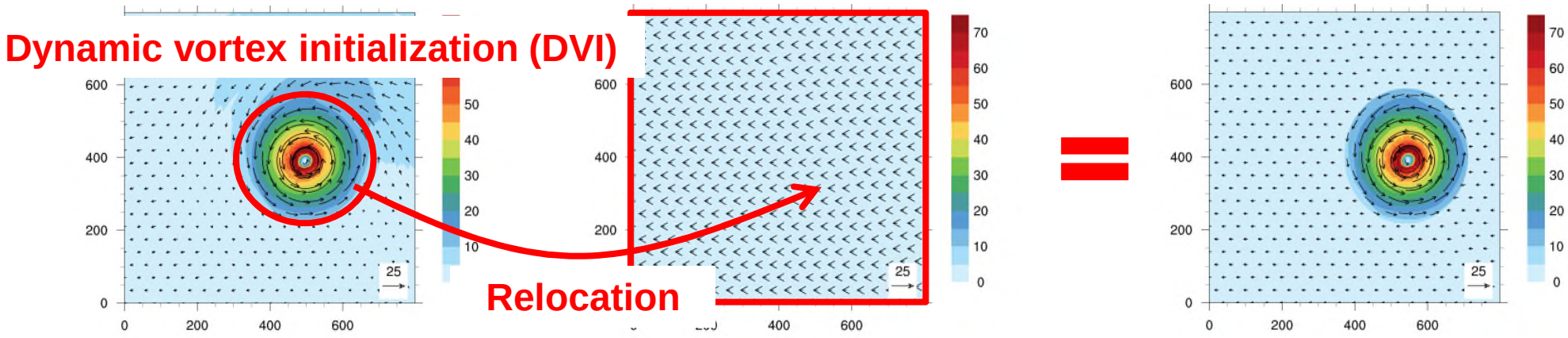

- Reducing spin-up time
- Minimizing the impact on the track during cyclone intensification

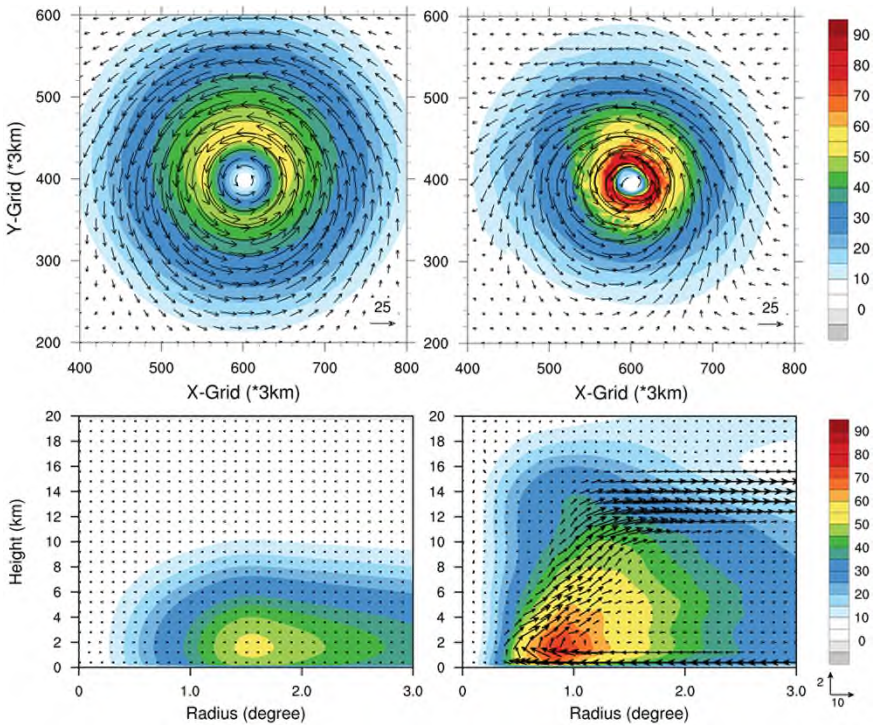

Result

0 ~ 36

A0

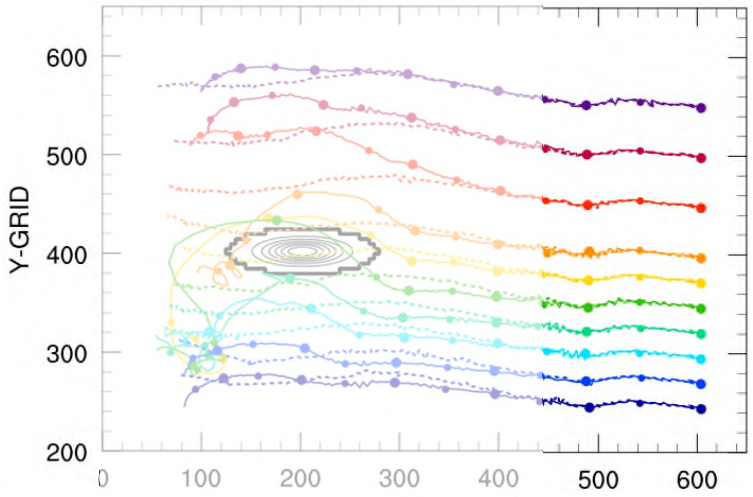

A45

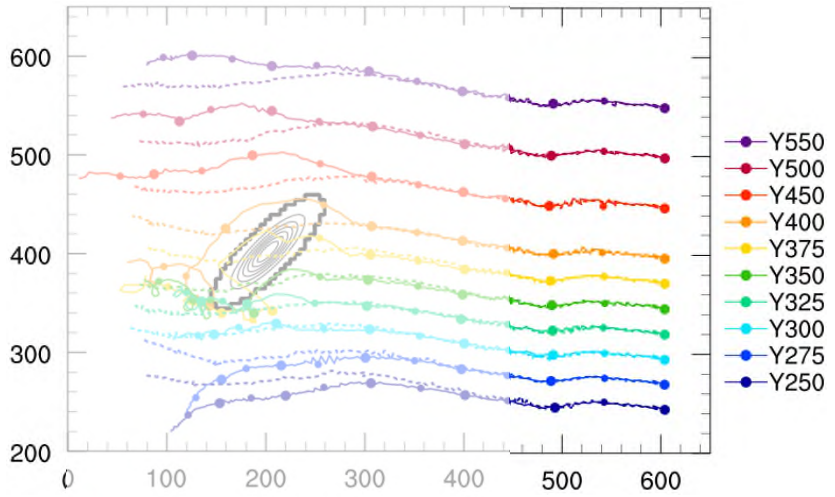

Cyclonic deflection

A90

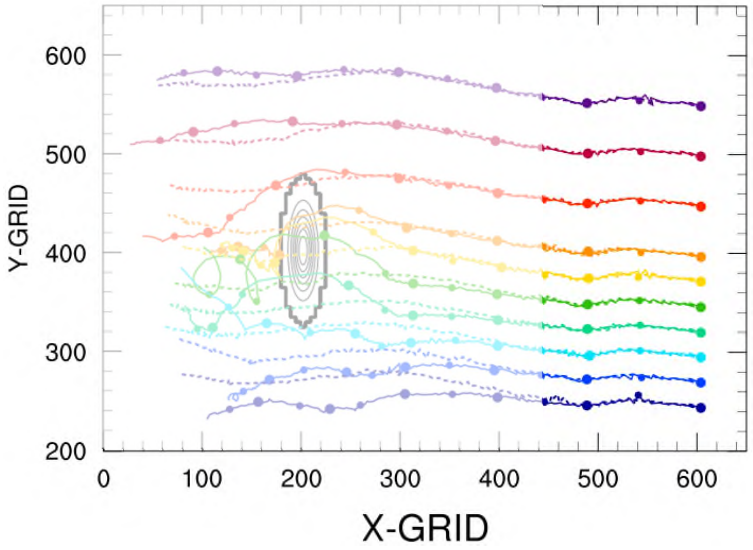

A135

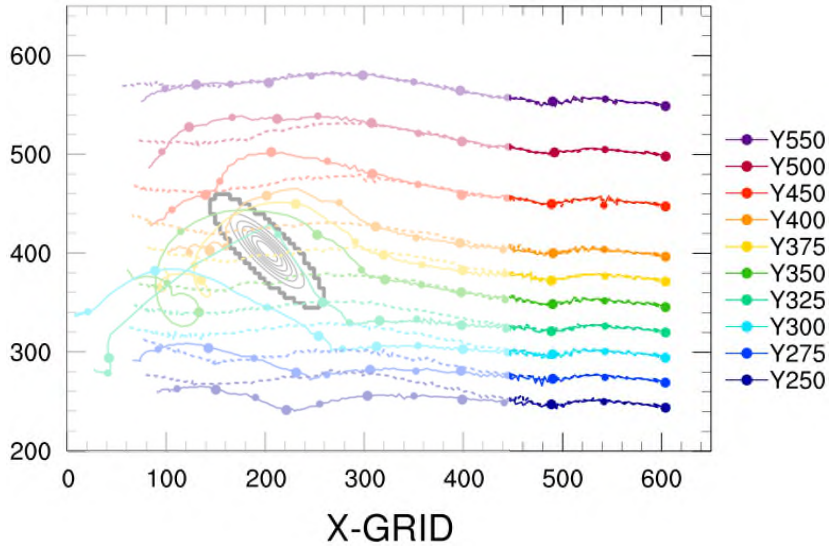

Result

- The stronger outer flow is separated by the terrain
- The flow r
  southeast
  the southerly wind

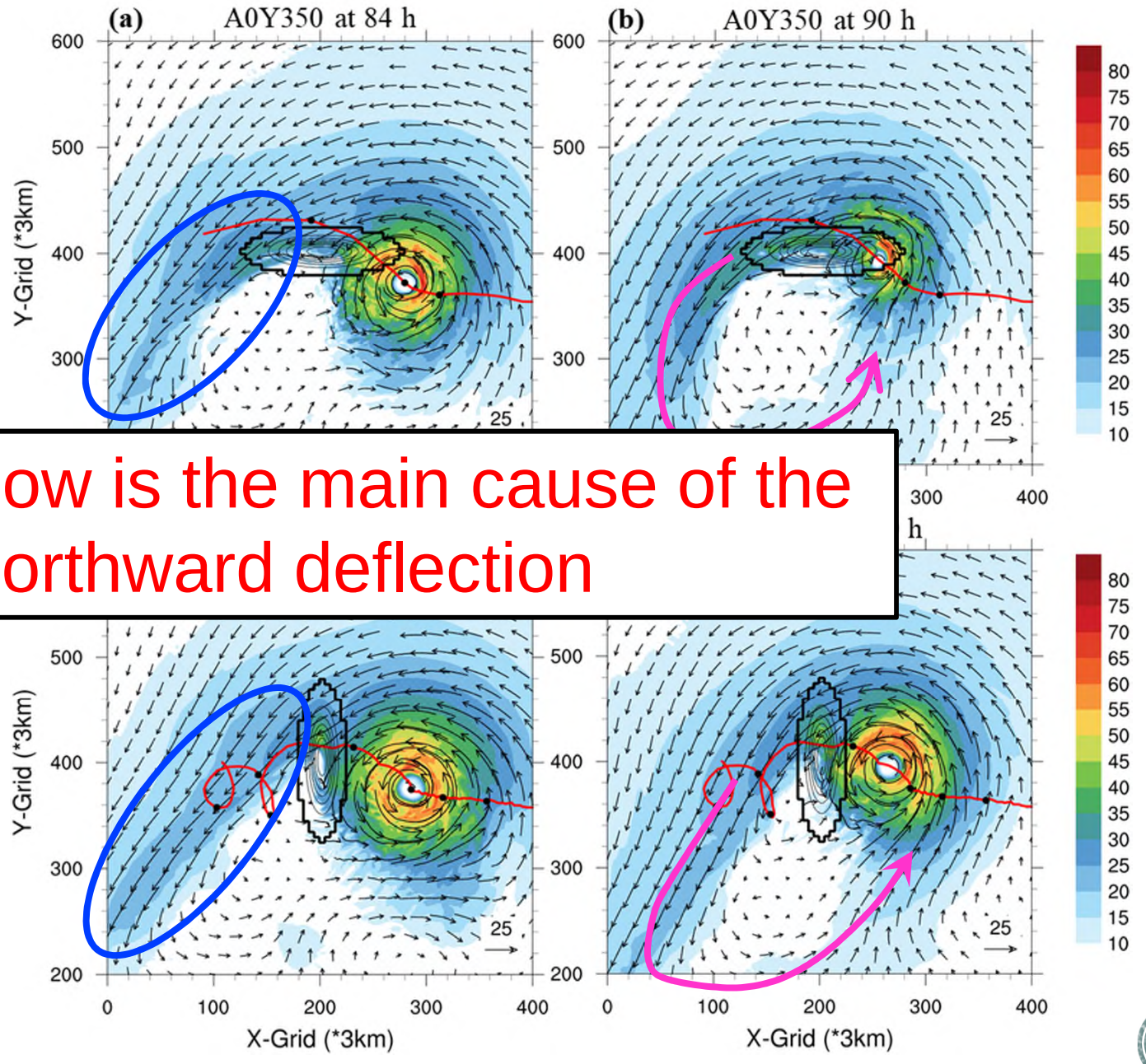

Recirculating flow is the main cause of the TC's northward deflection

Method

PV tendency analysis

Horizontal and vertical advection

$$\frac{\partial q}{\partial t} = -\boldsymbol{U}\cdot\nabla q + \left(\frac{\boldsymbol{\omega_a}}{\rho}\cdot\nabla\right)\frac{d\theta_v}{dt} + \nabla\theta_v\cdot\frac{\nabla\rho\times\nabla p}{\rho^3} + \frac{1}{\rho}\nabla\theta_v\cdot(\nabla\times\boldsymbol{F_r})$$

Tendency | Diabatic heating | Solenoidal | Friction

$$C_x = -\frac{\sum_{i=1}^{N}\left(\frac{\partial\bar{\zeta}_0}{\partial x}\right)_i\left(\frac{\partial\bar{\zeta}_1}{\partial t}\right)_i}{\sum_{i=1}^{N}\left(\frac{\partial\bar{\zeta}_0}{\partial x}\right)_i^2}, \qquad C_y = -\frac{\sum_{i=1}^{N}\left(\frac{\partial\bar{\zeta}_0}{\partial y}\right)_i\left(\frac{\partial\bar{\zeta}_1}{\partial t}\right)_i}{\sum_{i=1}^{n}\left(\frac{\partial\bar{\zeta}_0}{\partial y}\right)_i^2}$$

Wu and Wang (2000)

- Use Fourier transform to get vorticity budget wavenumber 1 (WN-1)
  (averaged in 1-8 km height in this study)
- Calculate TC translation speed and direction(Cx,Cy)
  (still has 1~2 m/s bias in this method)
- 3 main components : HA(horizontal advection)、VA(vertical advection)、DH(diabatic heating)

Result

- The majority of experiments are dominated by HA
- HA tends to deviate towards the right of the TC movement direction and gradually rotates southward over time (resulting cyclonic deflection)

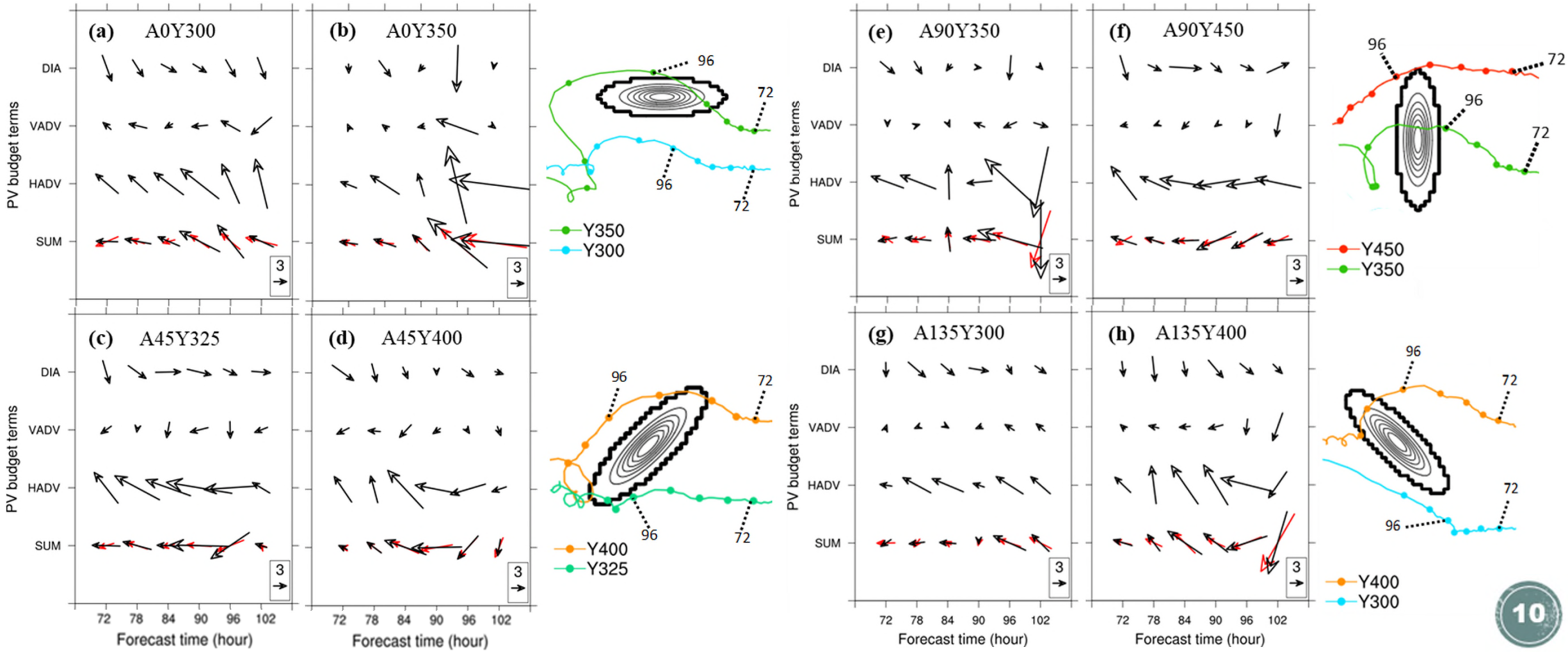

Result

WN-1 asymmetric wind (terrain – no terrain)

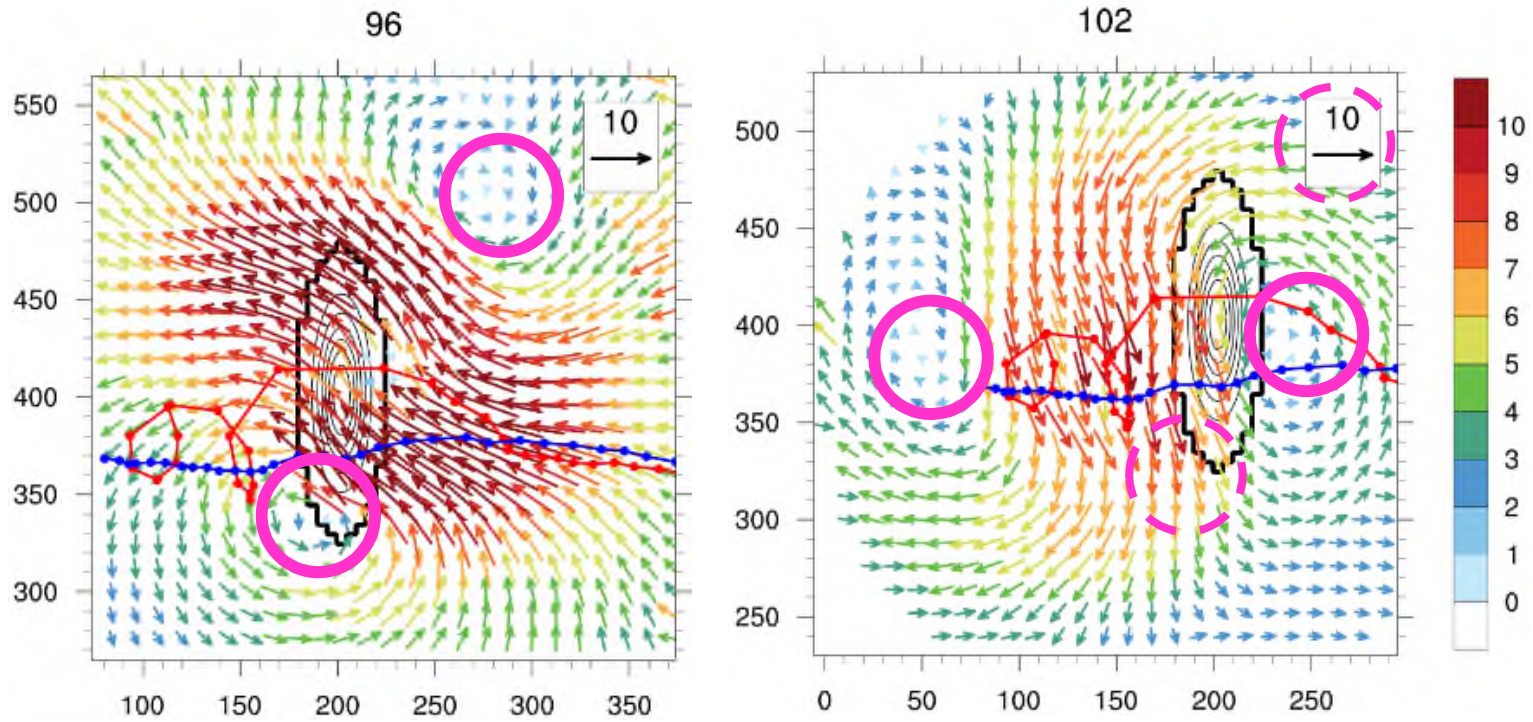

- A pair of gyres induced by the terrain effect on both sides of the TC

  (Tang and Chan, 2016b)
- Gyres also happen cyclonic deflection with track

Result

WN-1 asymmetric wind

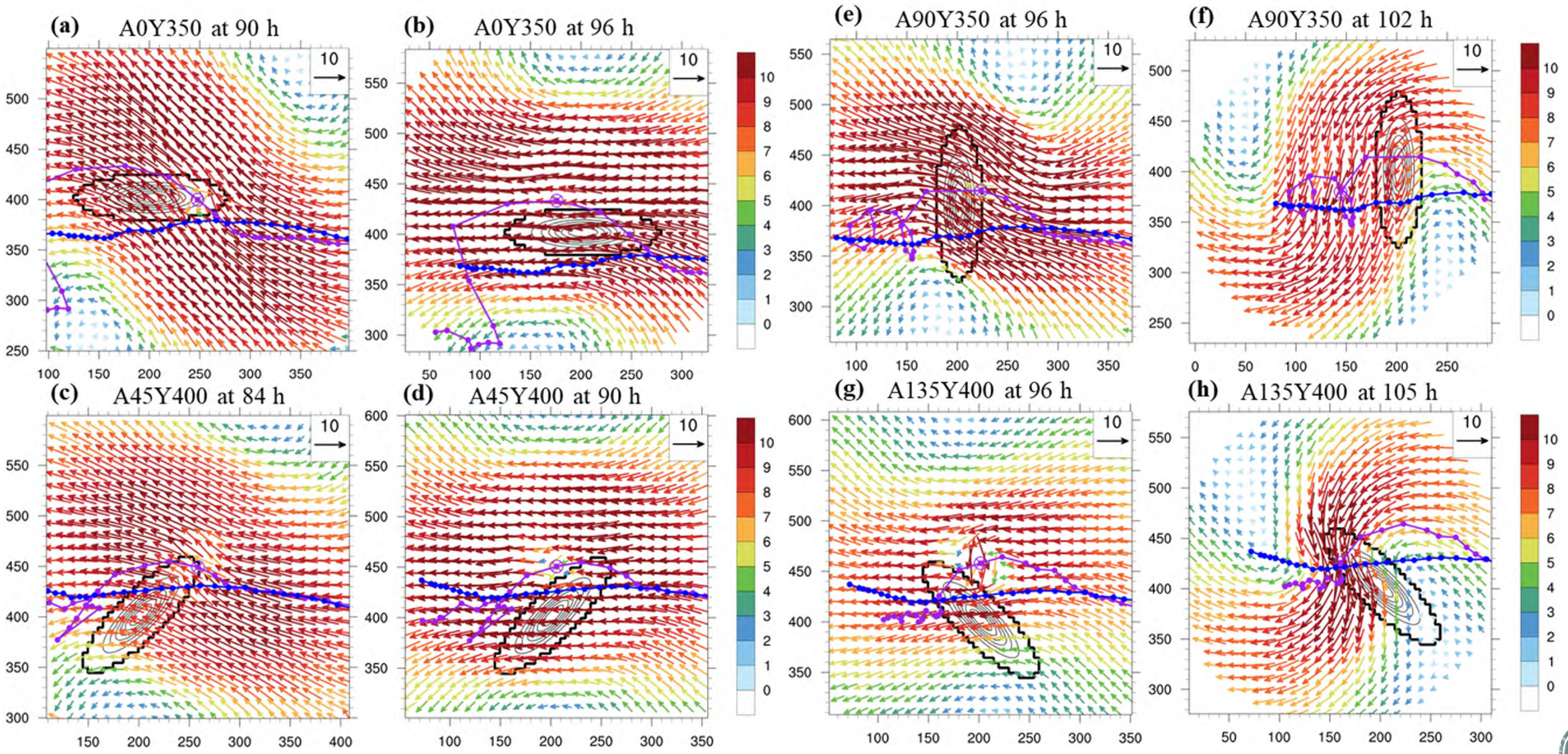

Result

Sensitivity experiment

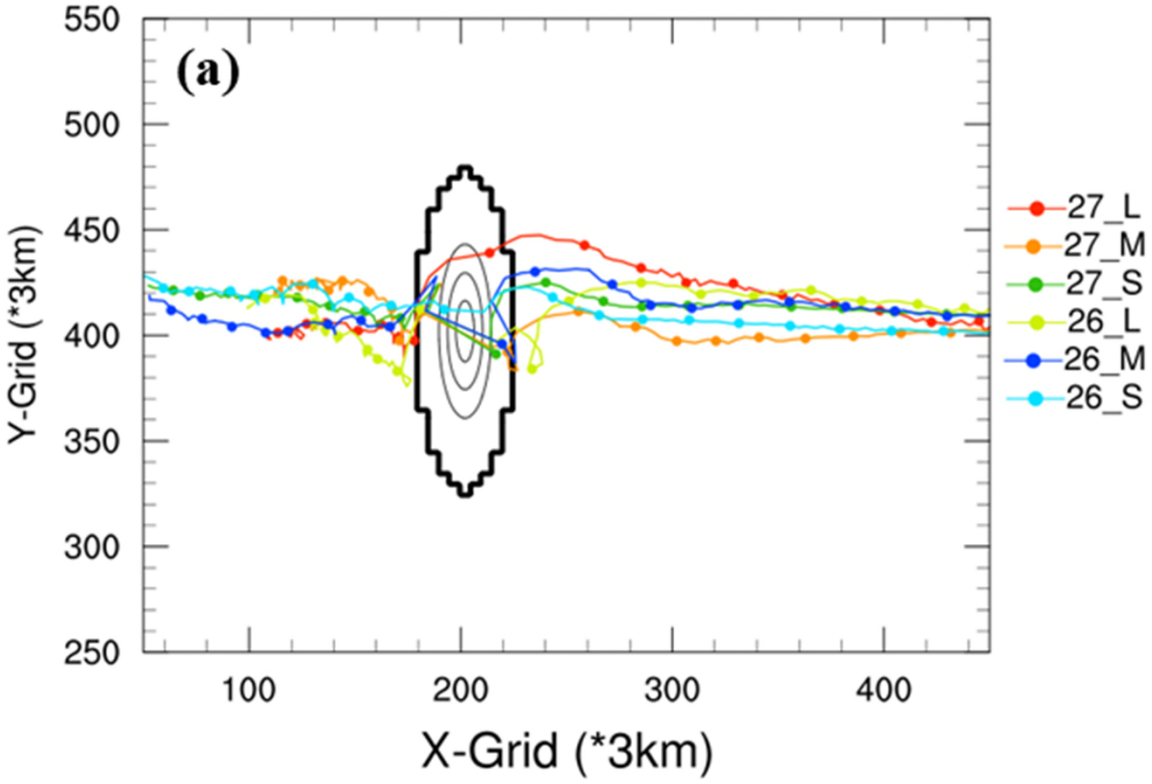

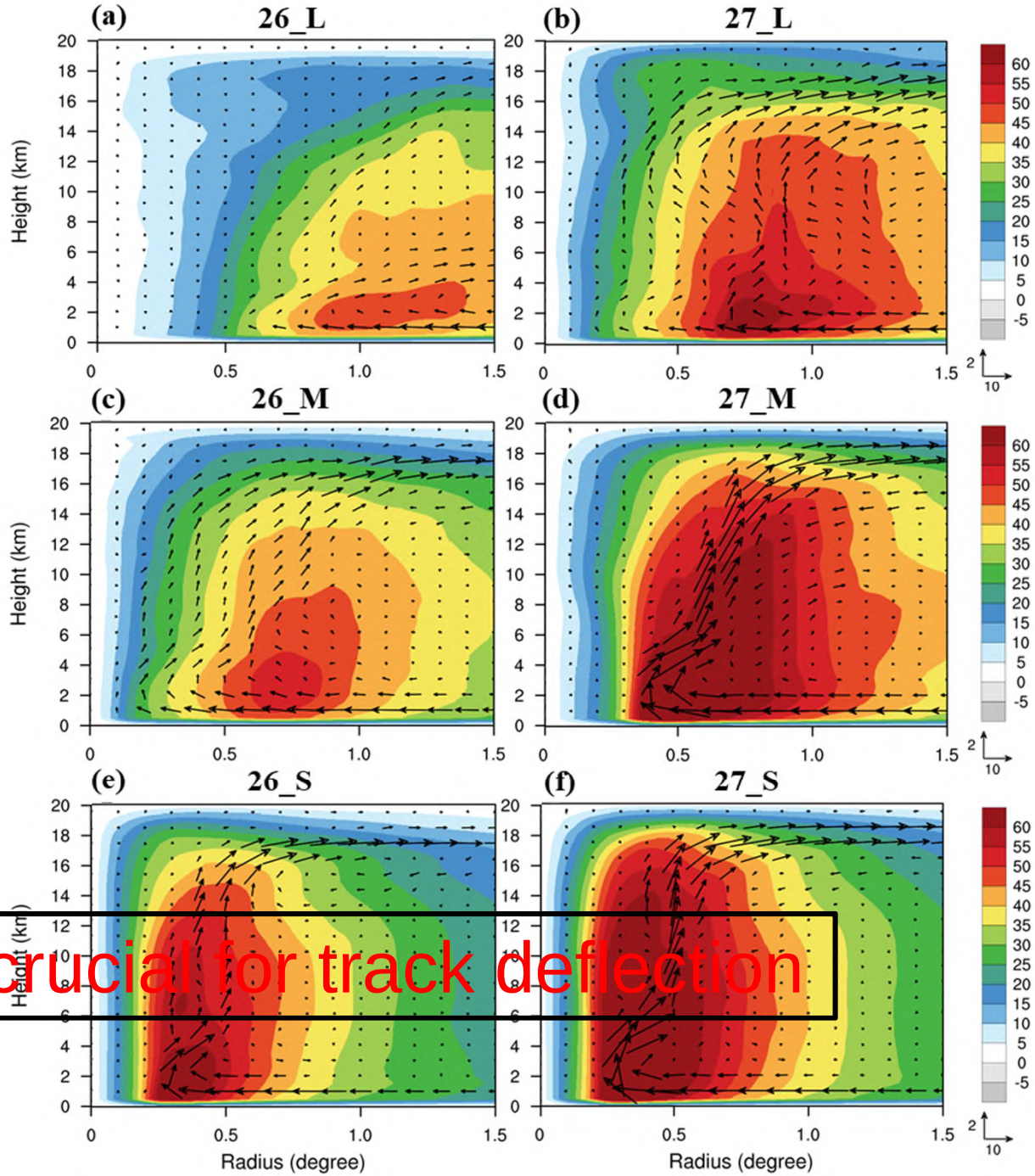

The size and structure are crucial for track deflection

Result

Sensitivity experiment

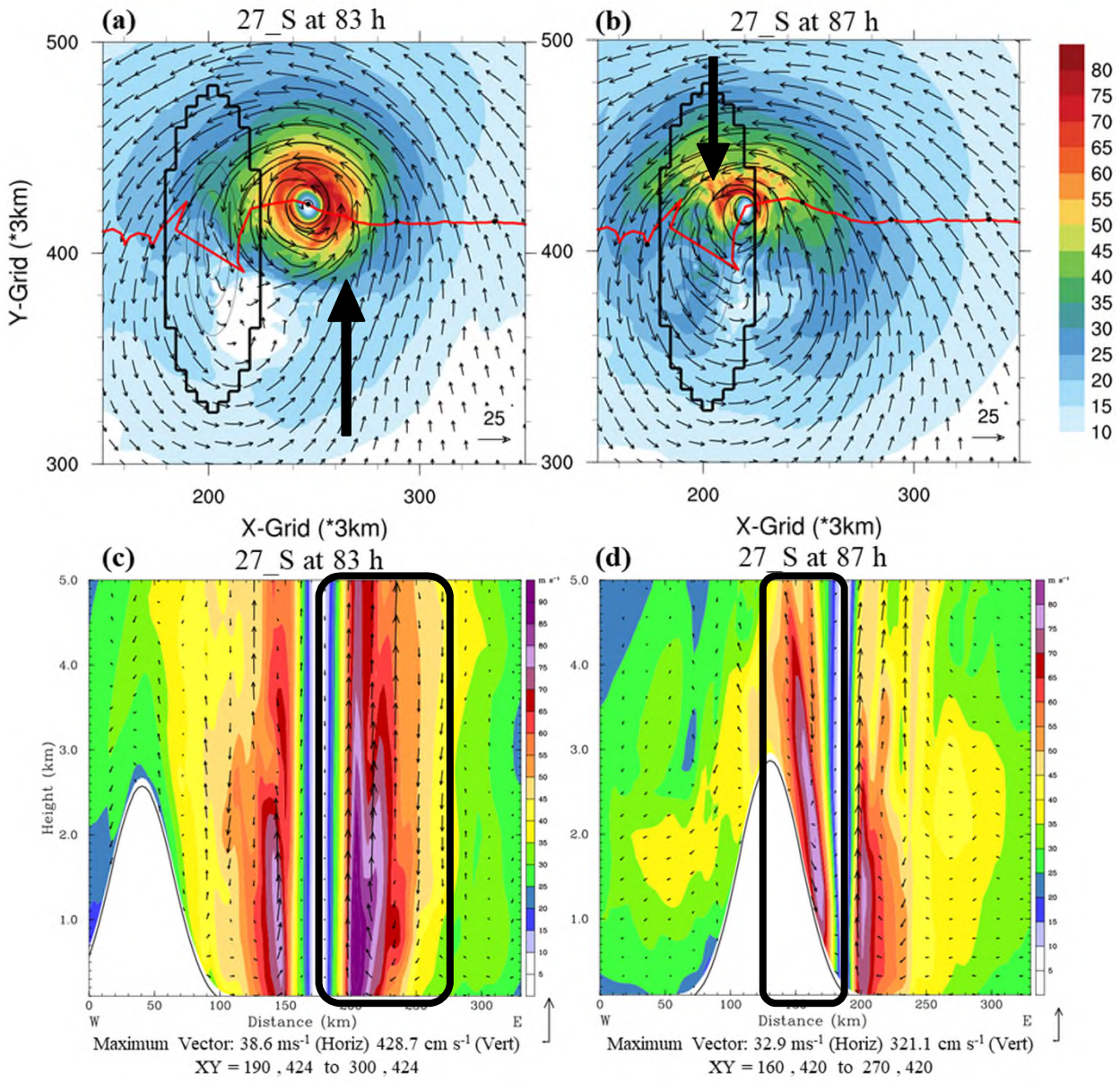

- Recirculating flow intensifies eastern winds (deflects northward)
- Stronger northerly jet over the eastern slope in the western quadrant of the inner TC vortex (channeling effect) (deflects southward)

Result

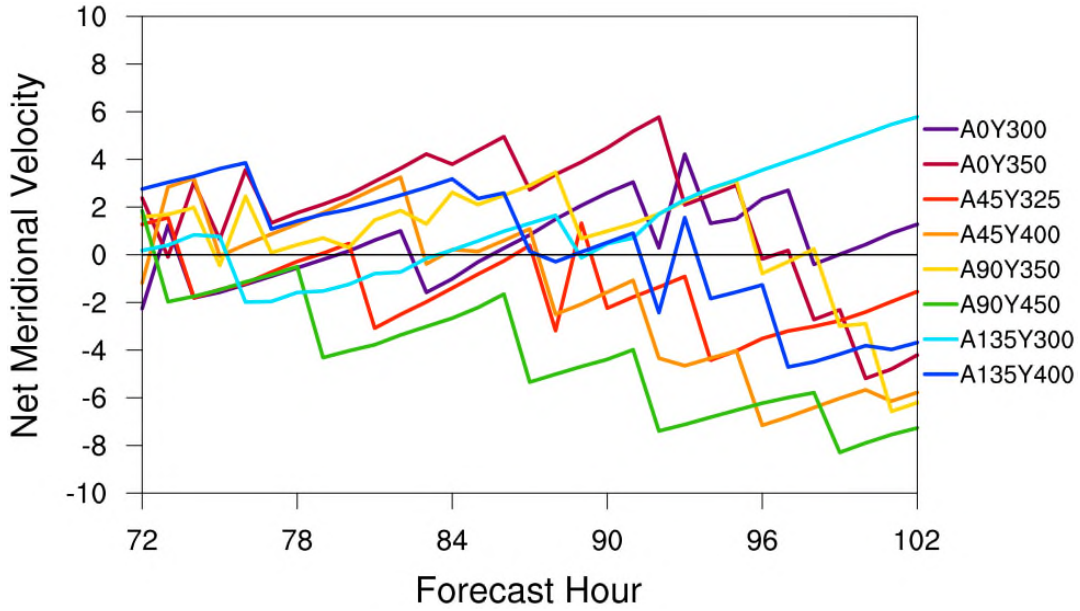

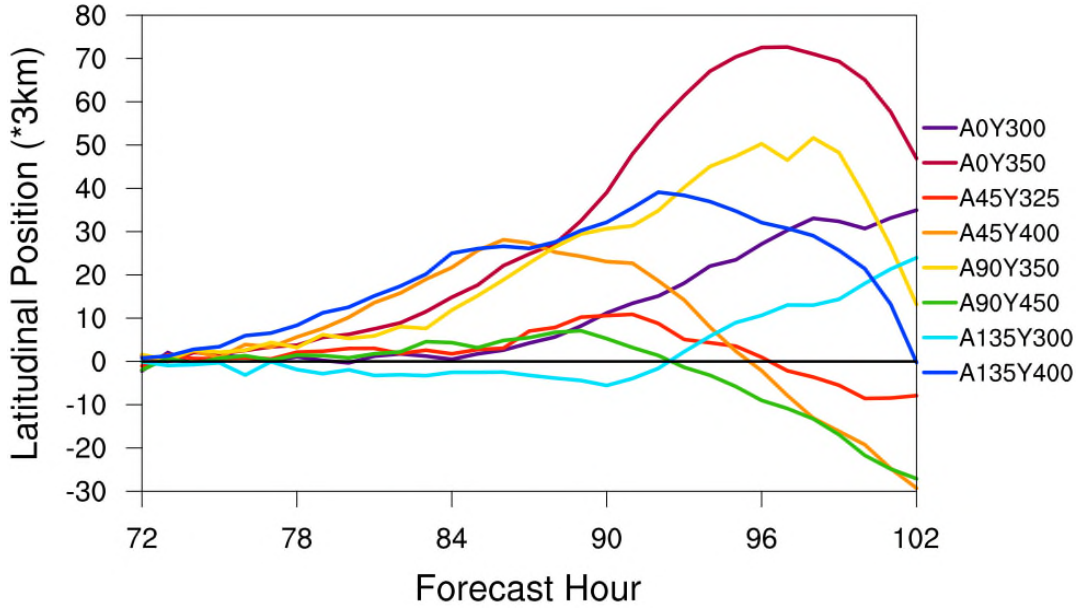

radius of 450 km of the TC averaged in 0-4 km height

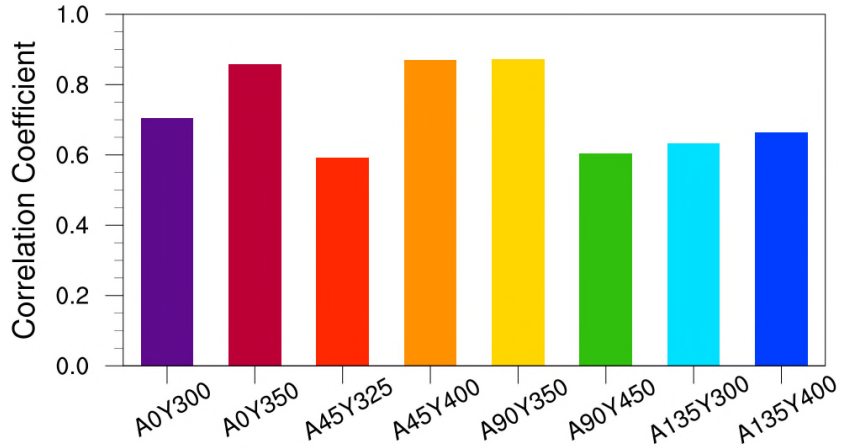

Sensitivity experiment

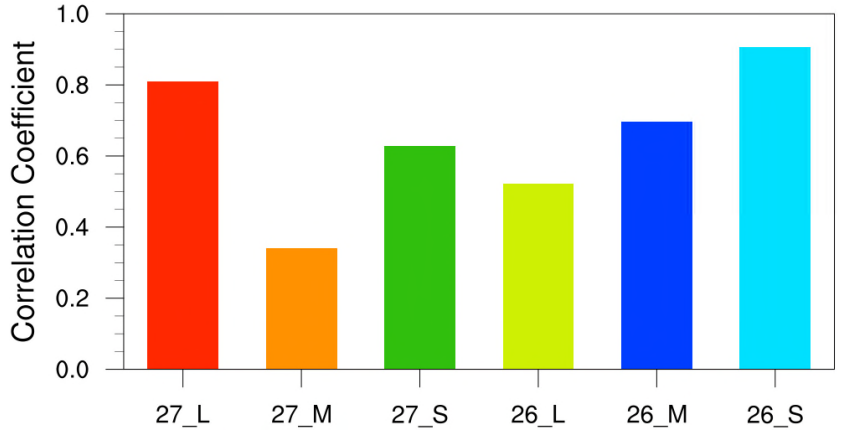

Method

Meridional wind budget analysis

terrain-following coordinates (x, y, σ)

zonal advection　　vertical advection　　Coriolis force

$$\frac{\partial v}{\partial t} = -u\left(\frac{\partial v}{\partial x} + \frac{\partial v}{\partial \sigma}\sigma_x\right) - v\left(\frac{\partial v}{\partial y} + \frac{\partial v}{\partial \sigma}\sigma_y\right) - w\frac{\partial v}{\partial \sigma}\sigma_z - \frac{1}{\rho}\left(\frac{\partial p'}{\partial y} + \frac{\partial p'}{\partial \sigma}\sigma_y\right) - fu + F_v$$

meridional advection　　pressure gradient force　　turbulent diffusion

- 4 main components : horizontal advection : hadv
  - zonal advection : hadv-u
  - meridional advection : hadv-v
  - vertical advection : vadv
  - pressure gradient force : pgf

(averaged in 0-4 km height in this study)

Result

27_L : not obvious

27_S : vadv strong

26_L : vadv week
pgf has effect

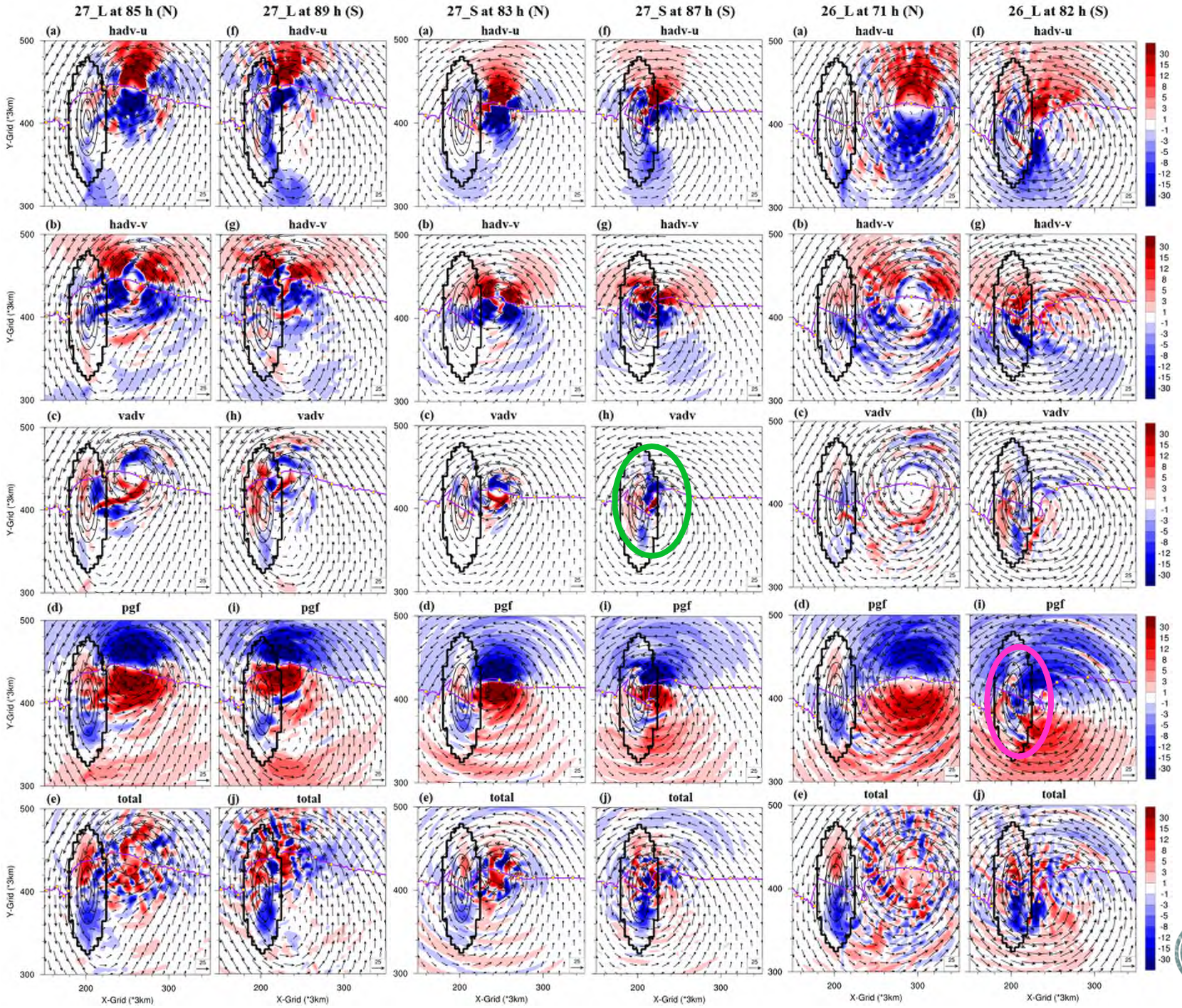

Result

Circulation analysis

- B (blocking and shading) : the flow of the TC affected by the terrain's obstruction
- R (Recirculating) : the flow types of the outer TC circulation passing over or around the lower part of the terrain
- C (Channeling) : "shading" is particularly strong near the slope the circulation is squeezed by the terrain

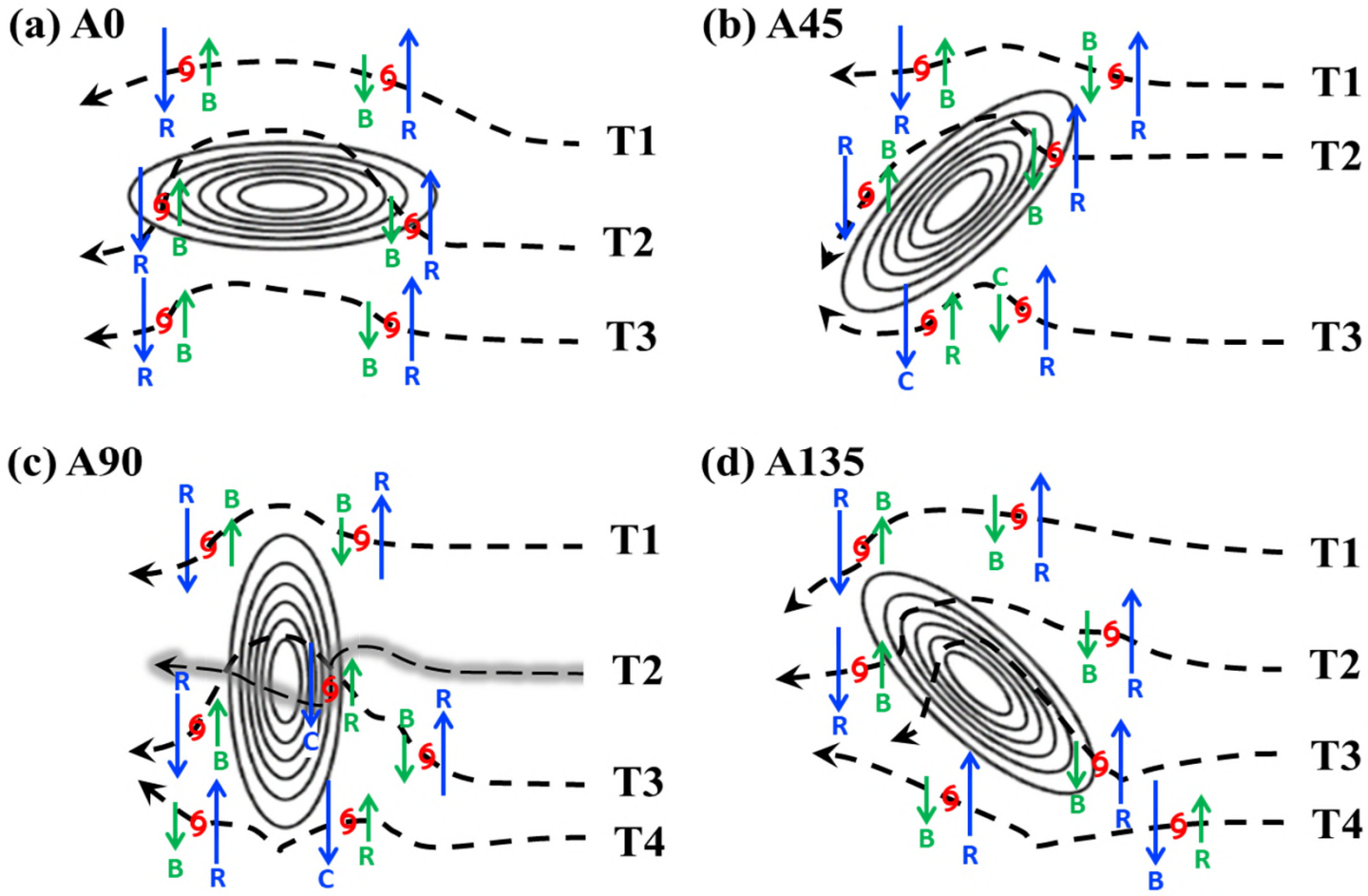

Conclusions

- The relative competition between the flow recirculating of the outer TC vortex and flow channeling of the inner TC vortex in inducing the track deflection of different incident TCs near the terrain.
- The PV budget analyses indicate that horizontal PV advection gives the major contribution to the TC movement.
- A pair of gyres in the WN-1 flow difference may be induced by the topographic effect, which take a counterclockwise rotation with time to facilitate the TC to deflect cyclonically. (as shown before but only for northwestward TC, Tang and Chan 2016b; Huang et al. 2022b)
- The dominance of the meridional velocity budget terms will depend on the relative competition between the effects of flow channeling and flow recirculating associated with the evolving asymmetric TC, which is related to the size of the RMW and the TC- incident quadrant of the terrain.
- This study has provided schematic diagrams of major flow types to regulate the track deflection of intense TCs near the terrain to net meridional flow steering for different terrain angles.

New Test

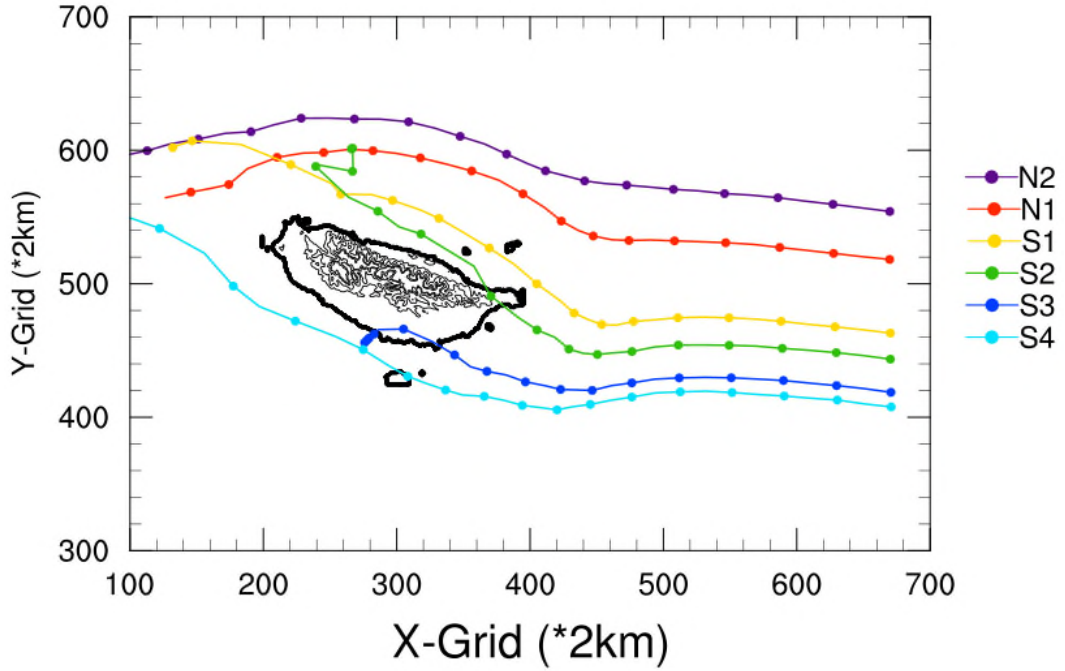

Resolution (nested domains)

D01 (601×601) : 10 km

D02 (1001×1001) : 2 km

f-plane : 23.5°

RMW = 75 km (initial for DVI)

S2

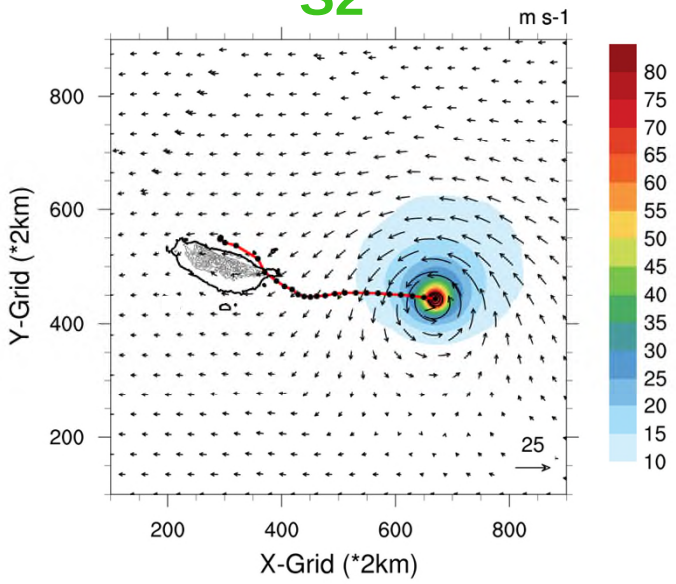

S3

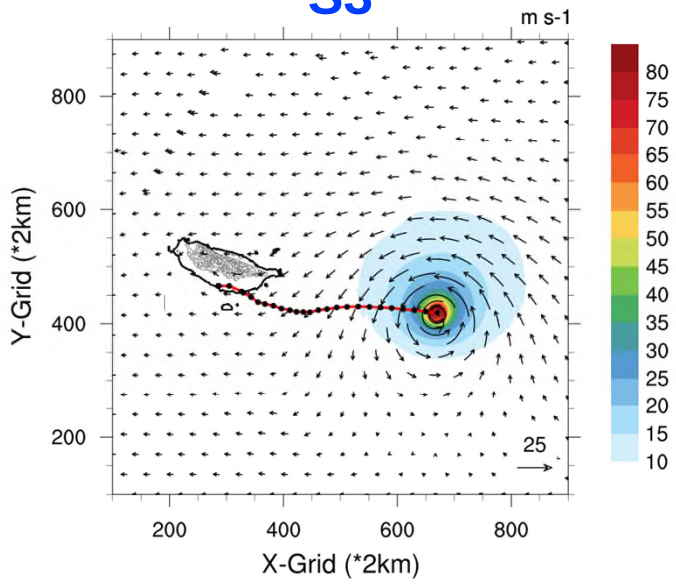

S4

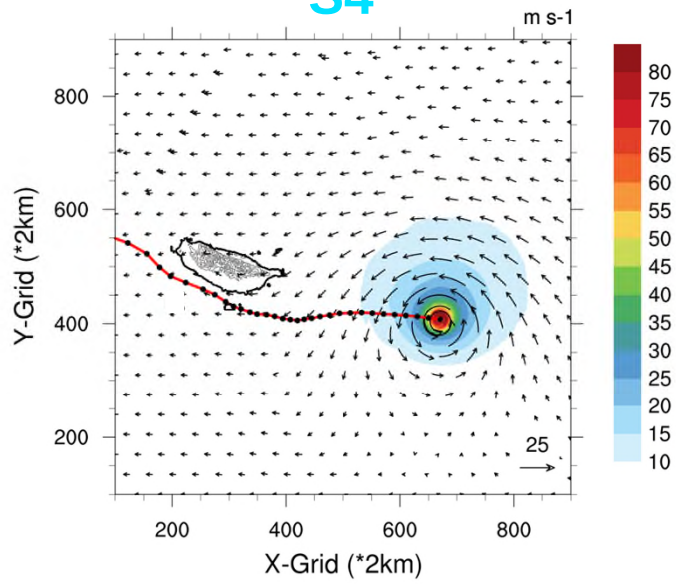

Result

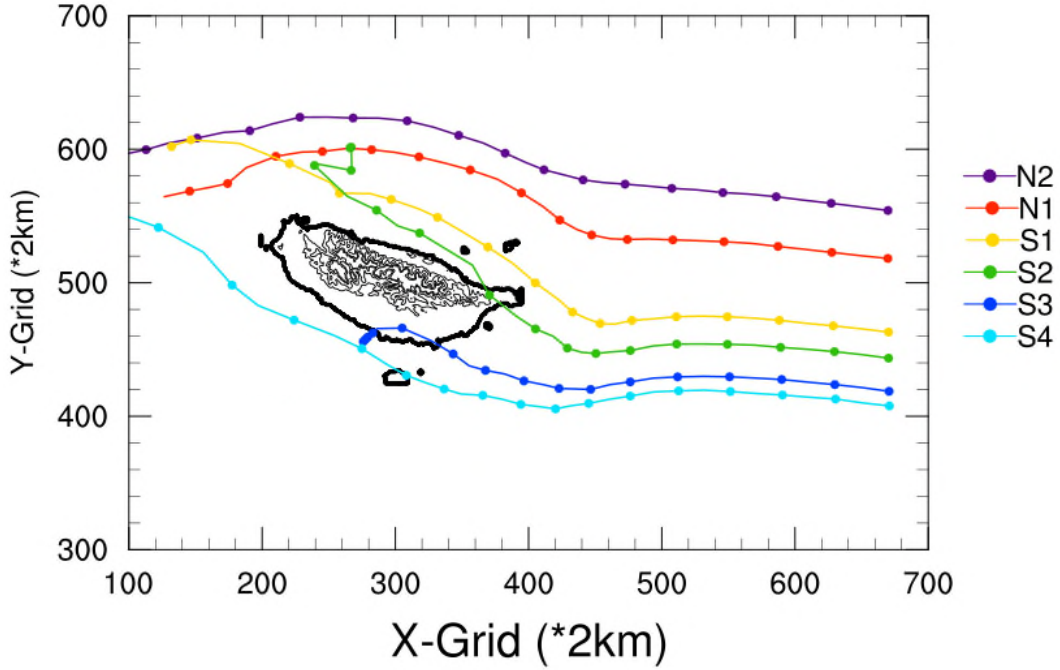

S2

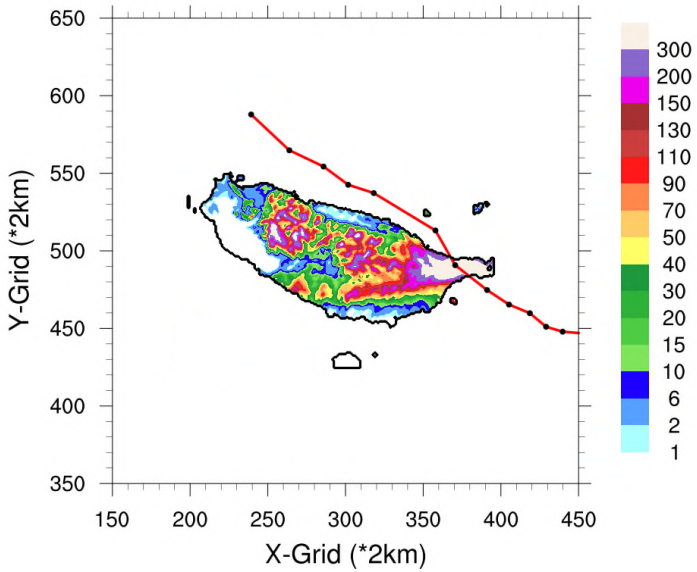

S3

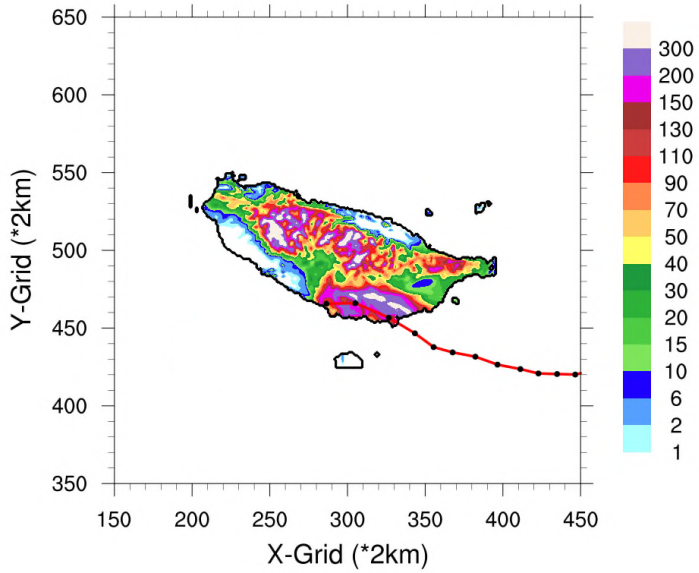

S4

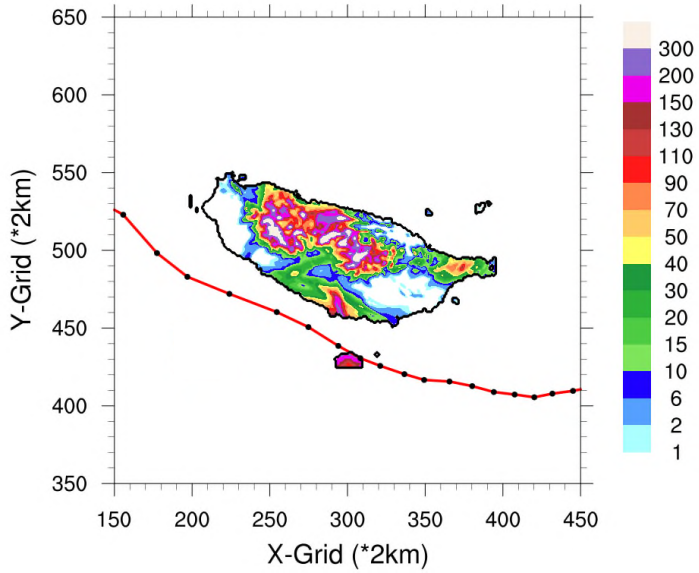

Result

S2

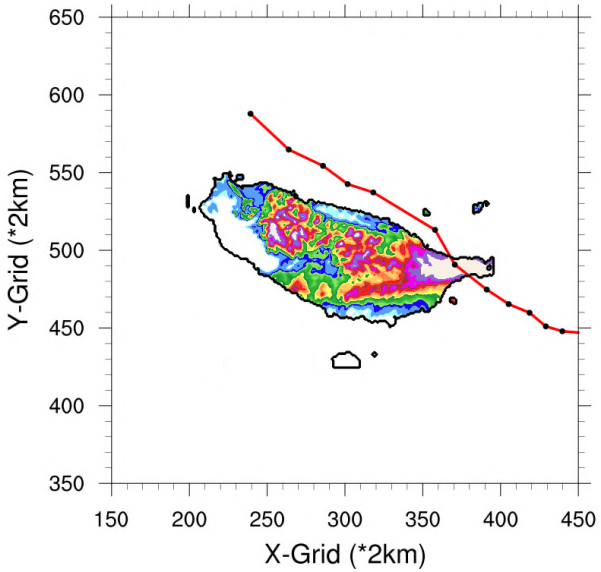
650
600
550
500
450
400
350
Y-Grid (*2km)
150
200
250
300
350
400
450
X-Grid (*2km)

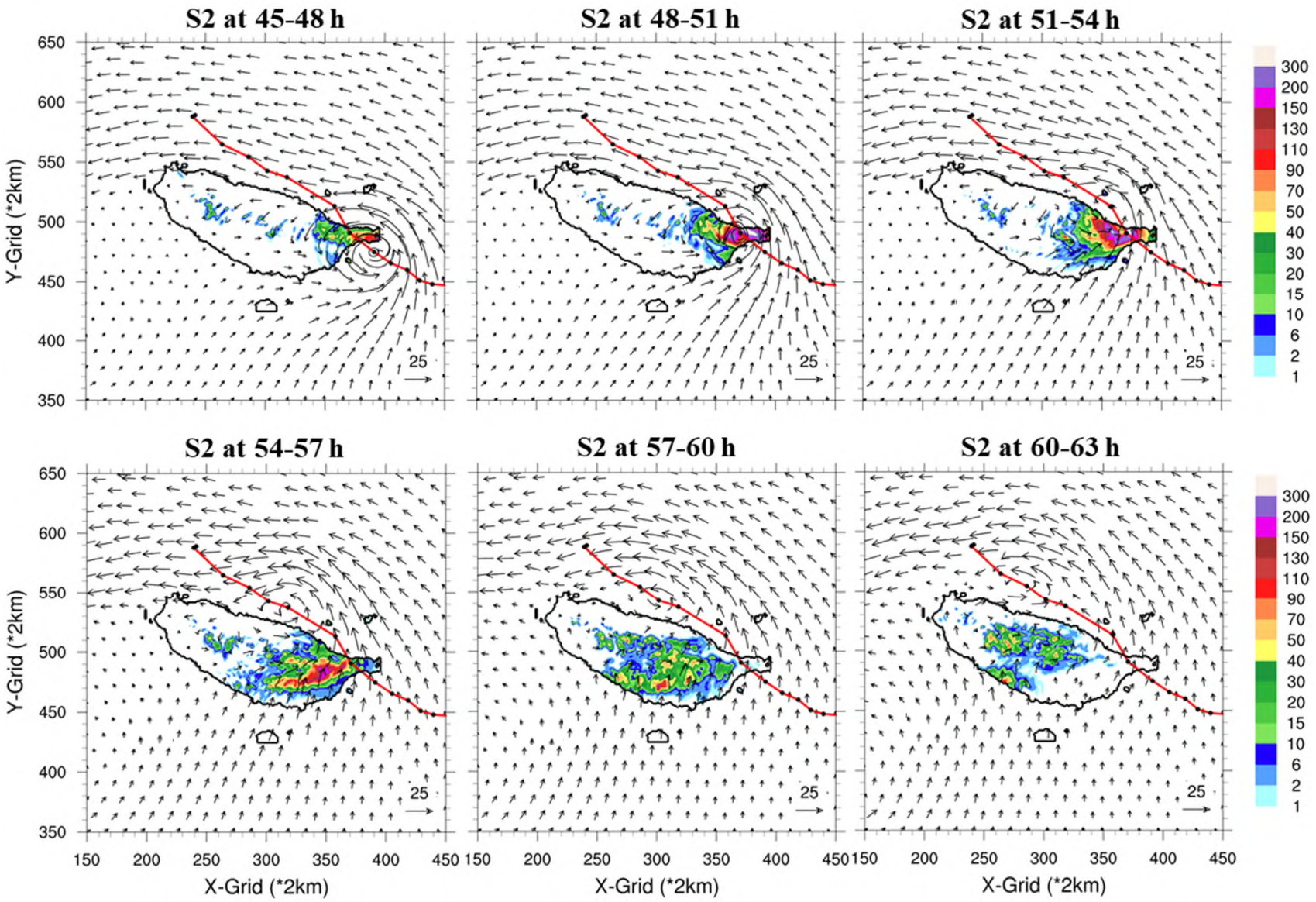
S2 at 45-48 h
S2 at 48-51 h
S2 at 51-54 h
S2 at 54-57 h
S2 at 57-60 h
S2 at 60-63 h
Y-Grid (*2km)
X-Grid (*2km)
650
600
550
500
450
400
350
150
200
250
300
350
400
450
25
300
200
150
130
110
90
70
50
40
30
20
15
10
6
2
1

Result

S3

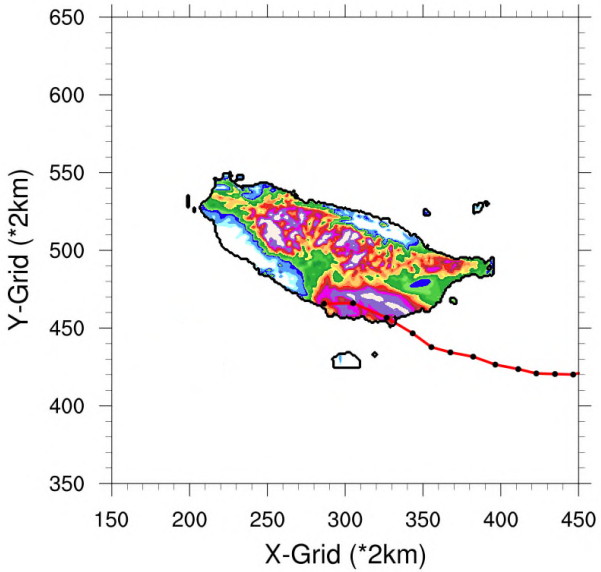
650
600
550
500
450
400
350
Y-Grid (*2km)
150
200
250
300
350
400
450
X-Grid (*2km)

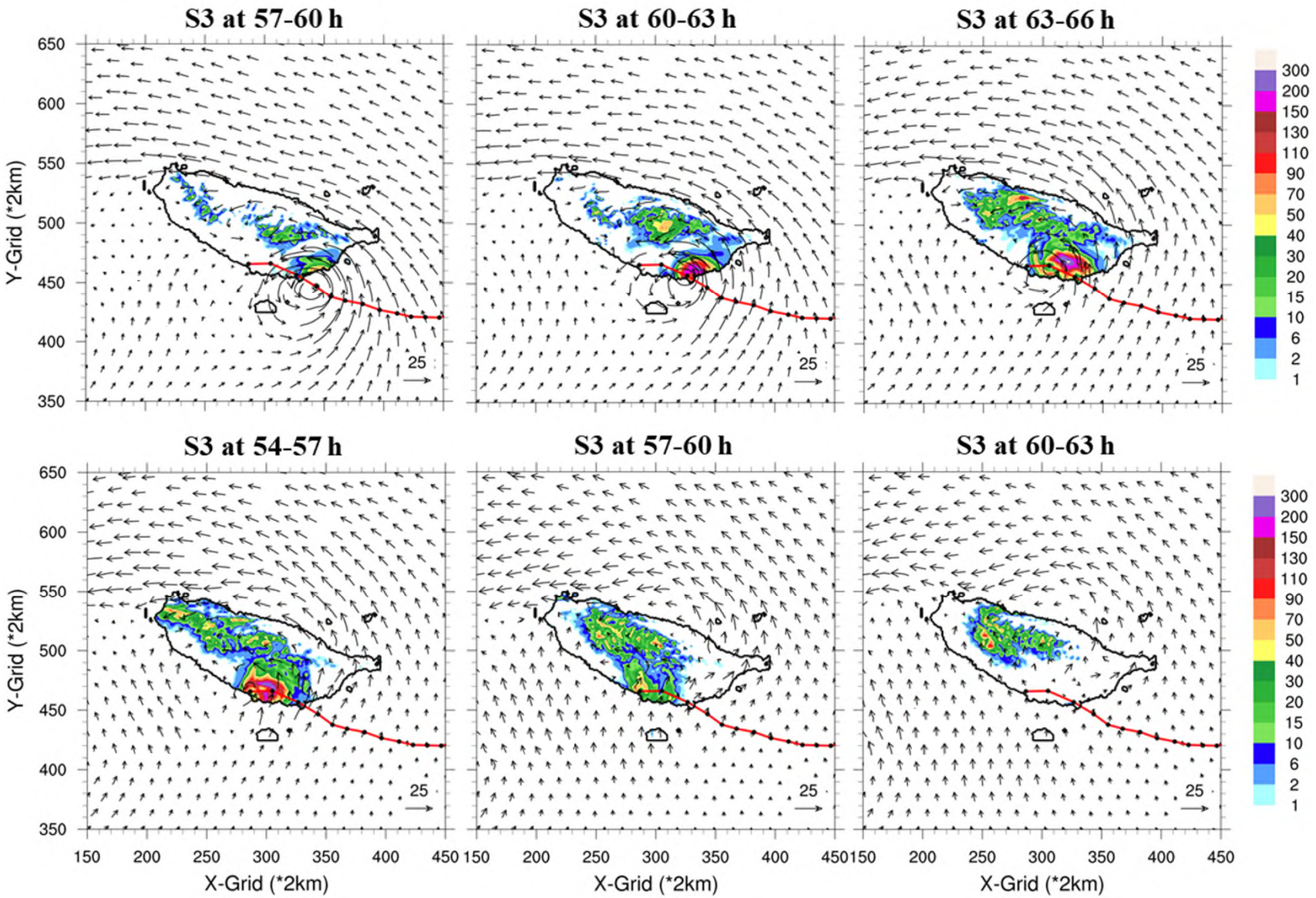
S3 at 57-60 h
S3 at 60-63 h
S3 at 63-66 h
S3 at 54-57 h
S3 at 57-60 h
S3 at 60-63 h
Y-Grid (*2km)
X-Grid (*2km)
25
300
200
150
130
110
90
70
50
40
30
20
15
10
6
2
1

Result

S4

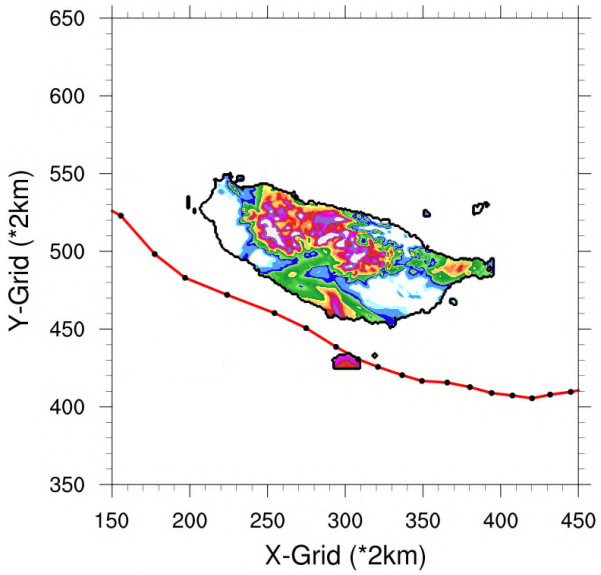
650
600
550
500
450
400
350
Y-Grid (*2km)
150
200
250
300
350
400
450
X-Grid (*2km)

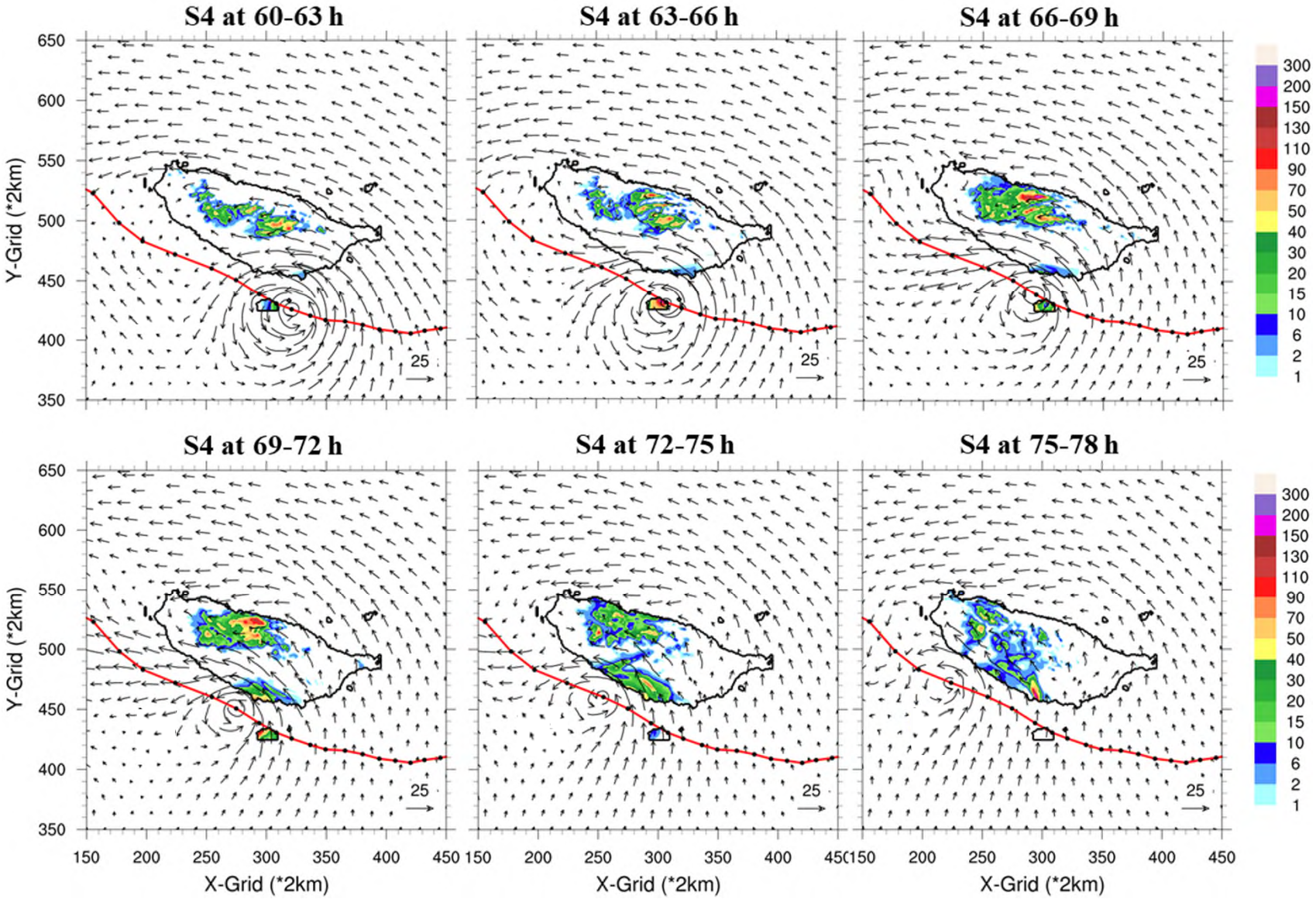
S4 at 60-63 h
S4 at 63-66 h
S4 at 66-69 h
S4 at 69-72 h
S4 at 72-75 h
S4 at 75-78 h
Y-Grid (*2km)
X-Grid (*2km)
650
600
550
500
450
400
350
150
200
250
300
350
400
450
25
300
200
150
130
110
90
70
50
40
30
20
15
10
6
2
1

Result

The contributions of ideal and real terrain are similar (hadv-u & hadv-v)

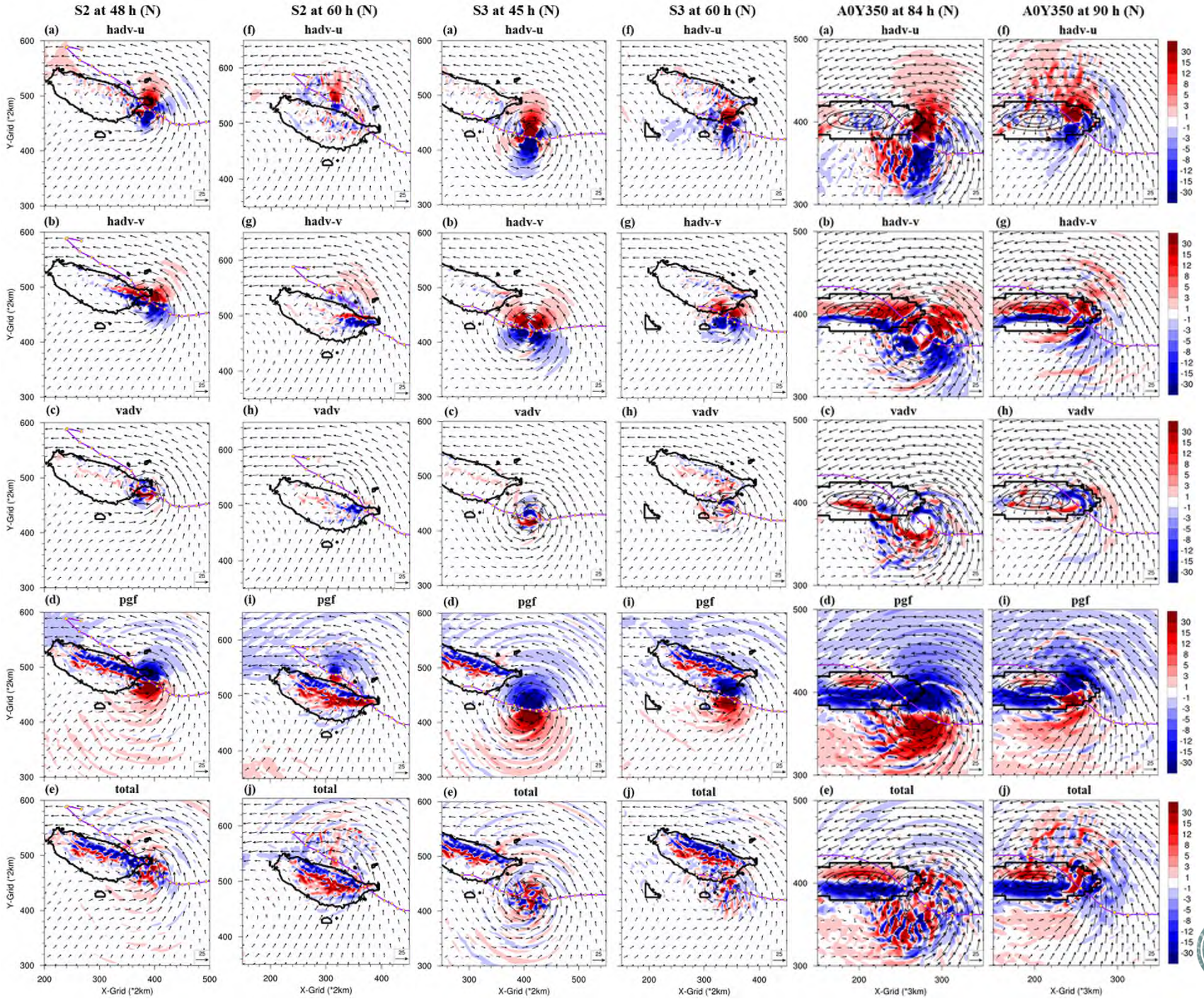

Reference

Hsu, L.-H., S.-H. Su, R. G. Fovell, and H.-C. Kuo, 2018: On typhoon track deflections near the east coast of Taiwan. *Mon. Wea. Rev.,* **146**, 1495–1510.

Huang, C.-Y., C.-A. Chen, S.-H. Chen, and D. S. Nolan, 2016: On the upstream track deflection of tropical cyclones past a mountain range: Idealized experiments. *J. Atmos. Sci*., **73,** 3157-3180.

Huang, K.-C., and C.-C. Wu, 2018: The imapct of idealized terrain on upstream tropical cyclone track. *J. Atmos. Sci.*, **75,** 3887–3910.

Huang, C.-Y.; Sha, S.-H.; Kuo, H.-C., 2022: A modeling study of Typhoon Lekima (2019) with the topographic influence of Taiwan. *Mon. Wea. Rev.,* **150**, 1993–2011.

Jian, G.-J., and C.-C. Wu, 2008: A numerical study of the track deflection of Supertyphoon Haitang (2005) prior to its landfall in Taiwan. *Mon. Wea. Rev*., **136**, 598-615.

Reference

Kuo, H.-C., R.T. Williams, J.-H. Chen, and Y.-L. Chen, 2001: Topographic effects on barotropic vortex motion: No mean flow. *J. Atmos. Sci*., **58**, 1310–1327.

Tang, C.-K., and J.C.-L. Chan, 2016b: Idealized simulations of the effect of Taiwan topography on the tracks of tropical cyclones with different steering flow strengths, *Q. J. R. Meteorol. Soc*. **142**: 3211–3221.

Wu, C.-C., T.-H. Li, and Y.-H. Huang, 2015: Influence of mesoscale topography on tropical cyclone tracks: Further examination of the channeling effect. *J. Atmos. Sci*., **72**, 3032–3050.

Wu, L., and B. Wang, 2000: A potential vorticity tendency diagnostic approach for tropical cyclone motion. *Mon. Wea. Rev.*, **128**, 1899-1911

Yeh, T.-C., and R.L., Elsberry, 1993: Interaction of typhoons with the Taiwan orography. Part I: upstream track deflection. *Mon. Wea. Rev.*, **121**, 3193-3212.

Thanks for listening !

Introduction

Using dynamic vortex initialization (DVI) method to reduce forecasting error

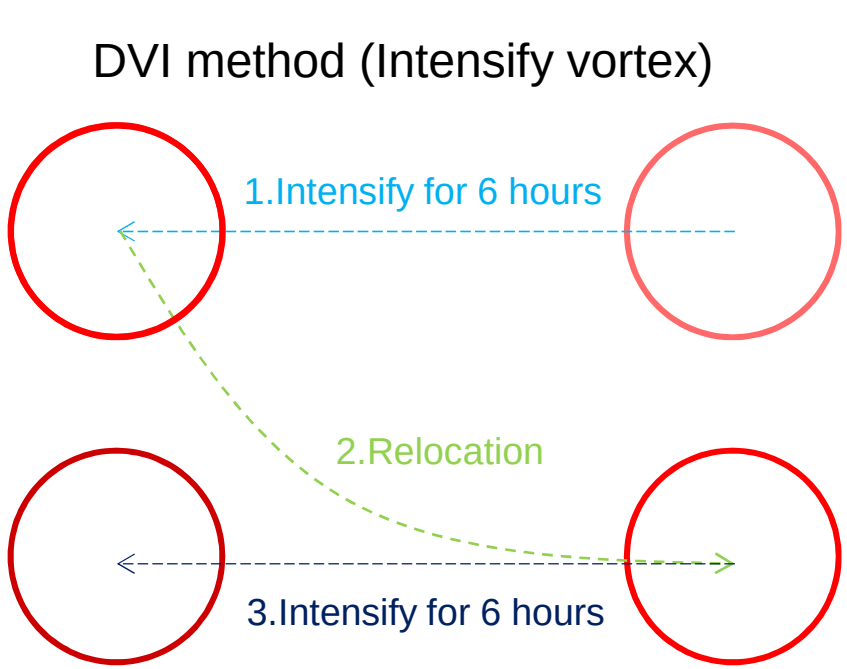

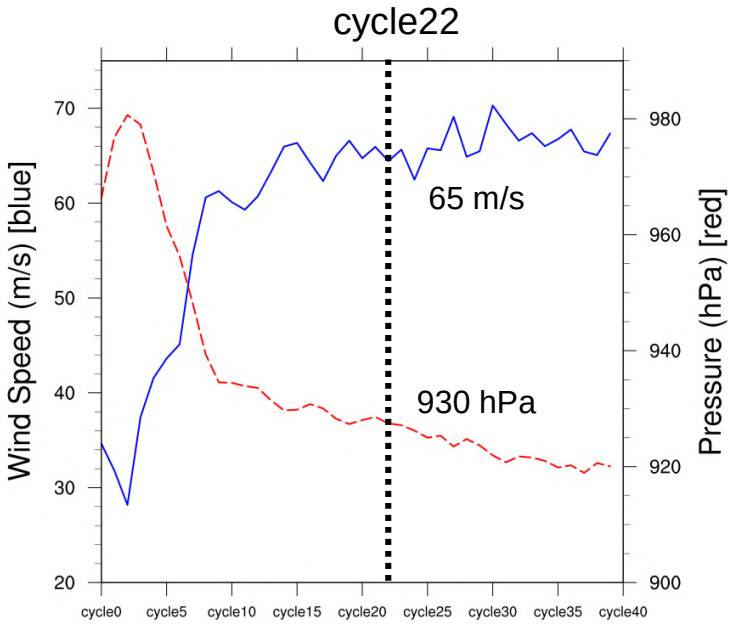

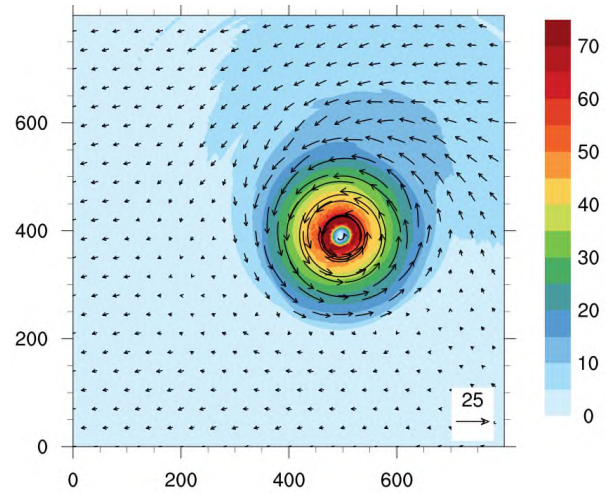

Result

Circulation analysis

A0-Y350

- The northwest side flow is obstructed by the terrain and can only bypass it
- The split flow join in the southeastward flow of the cyclone and intensify the convergence in the east of the cyclone
- It is beneficial to the development of convection on the eastern side, increasing the asymmetry of the cyclone's structure and helping the cyclonic deflection

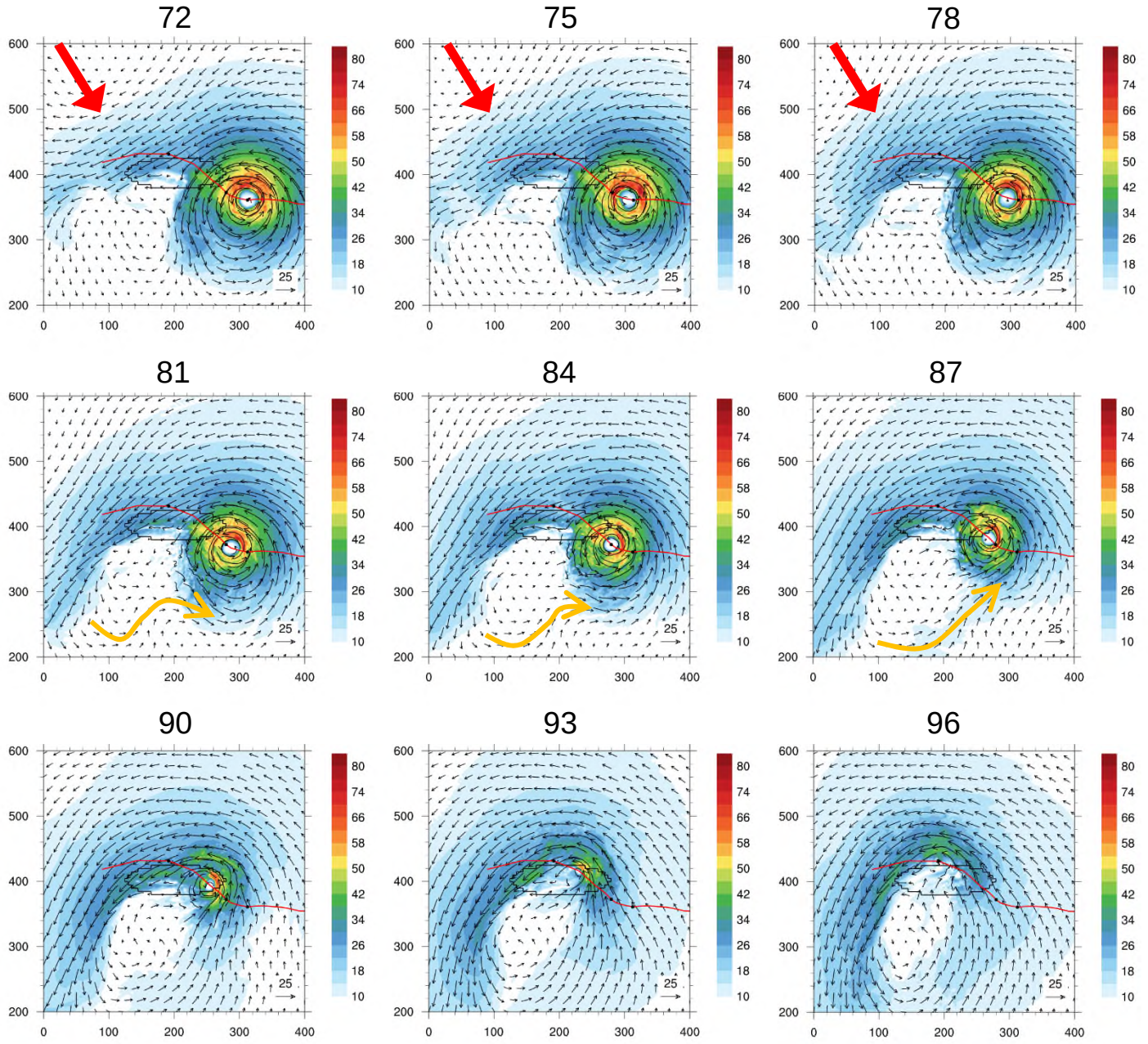

1.5 km high circulation(shaded, m/s^{-1})
1.5 km high wind(vector, m/s^{-1})

red line : track
black dot : every 12 hours for track position

Result

Contoured frequency by altitude diagrams (CFAD) of meridional wind velocity within the radius of 450 km